Perturbing integrin function inhibits microtubule growth from centrosomes, spindle assembly, and cytokinesis

Carlos G. Reverte, Angela Benware, Christopher W. Jones, and Susan E. LaFlamme

Center for Cell Biology and Cancer Research, Albany Medical College, Albany, NY 12208

In many mammalian cell types, integrin-mediated cell-matrix adhesion is required for the G1–S transition of the cell cycle. As cells approach mitosis, a dramatic remodeling of their cytoskeleton accompanies dynamic changes in matrix adhesion, suggesting a mechanistic link. However, the role of integrins in cell division remains mostly unexplored. Using two cellular systems, we demonstrate that a point mutation in the β1 cytoplasmic domain (β1 tail) known to decrease integrin activity supports entry into mitosis but inhibits the assembly of a radial microtubule array focused at the centrosome during interphase, the formation of a bipolar spindle at mitosis and cytokinesis. These events are restored by externally activating the mutant integrin with specific antibodies. This is the first demonstration that the integrin β1 tail can regulate centrosome function, the assembly of the mitotic spindle, and cytokinesis.

Introduction

Many types of mammalian cells require adhesion to the extracellular matrix to proliferate (Assoian and Schwartz, 2001). Integrins are the major family of receptors that mediate cell-matrix adhesion (Hynes, 2002). It is well established that integrins synergize with growth factor receptors to promote the G1–S transition of the cell cycle (Assoian and Schwartz, 2001). Progression through the cell cycle is accompanied by changes in adhesive interactions with the extracellular matrix and the remodeling of the actin and microtubule (MT) cytoskeletons (Glotzer, 2001). During interphase, integrins cluster at matrix contacts called focal adhesions (FAs; Geiger et al., 2001). Actin filaments organize in stress fibers that terminate at FAs, and MTs radiate from the centrosome to the cell cortex (Vandre et al., 1984; Geiger et al., 2001). As mitosis begins, cells loosen attachments; disassemble FAs, stress fibers, and MTs; and adopt a round morphology (Maddox and Burridge, 2003). MTs then reassemble into the bipolar spindle to direct accurate segregation of genetic material, and actin filaments form the contractile ring to separate daughter cells during cytokinesis (Vandre et al., 1984; Glotzer, 2001). As cell division nears completion, daughter cells respread and FAs, stress fibers, and the radial MT network are reformed. This dynamic regulation of adhesion during cell division suggests a mechanistic link. A requirement for matrix adhesion for the division of some cell types was reported more than two decades ago (Orly and Sato, 1979; Ben-Ze'ev and Raz, 1981; Winklbauer, 1986). In addition, β1-null chondrocytes exhibit a high incidence of binucleation, suggesting that β1 integrins regulate cytokinesis in this cell type (Aszodi et al., 2003). Here, we report that a mutation in the integrin β subunit cytoplasmic domain (β tail) that suppresses integrin activation allows entry to mitosis but inhibits the assembly of MTs from the centrosome and disrupts cytokinesis by preventing the formation of a normal bipolar spindle. We further demonstrate that the addition of an antibody, which activates the mutant integrin, restores centrosome function, bipolar spindle assembly, and cytokinesis. This is the first demonstration that the integrin β1 tail can regulate centrosome function, spindle formation, and cytokinesis.

Results and discussion

The conserved membrane-proximal NPXY motif in the β1 tail regulates integrin activation (O'Toole et al., 1995; Bodeau et al., 2001). To test whether this motif is required for cell proliferation, we generated CHO cell lines stably expressing either a wild-type (WT) β1 tail or a mutant β1 tail with an alanine substitution at tyrosine 783 within the NPIY motif

Correspondence to Susan E. LaFlamme: laflams@mail.amc.edu

Abbreviations used in this paper: FA, focal adhesion; Fg, fibrinogen; Fn, fibronectin; Lm, laminin-1; MT, microtubule; WT, wild-type.

The online version of this article contains supplemental material.

The Journal of Cell Biology, Vol. 174, No. 4, August 14, 2006 491–497
http://www.jcb.org/cgi/doi/10.1083/jcb.200603069

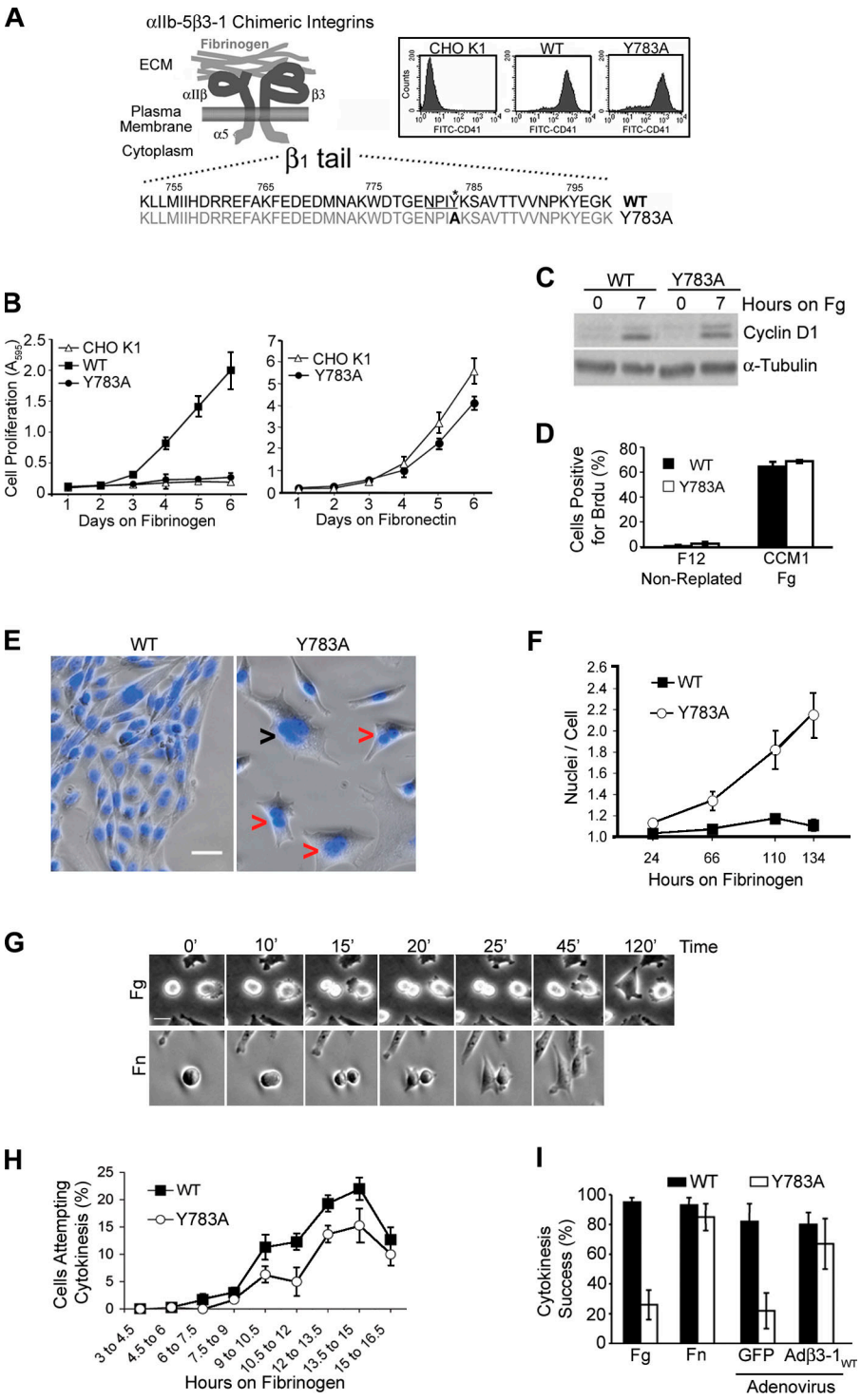

Figure 1. **Alanine substitution for tyrosine 783 in the β1 tail inhibits cell proliferation by inhibiting cytokinesis.** (A) The αIIb-5β3-1 heterodimeric chimeric integrins are depicted with the amino acid sequences of the WT and Y783A mutant β1 tails. Alanine (bold) is substituted for tyrosine 783 (asterisk) within the NPIY motif (underlined). (Inset) analysis of surface expression of chimeric integrin (CD41-FITC signal) in WT and Y783A cells by flow cytometry. CHO K1 cells were used as a negative control. (B) The Y783A mutation inhibits cell proliferation on Fg but not on Fn. CHO K1, WT, and Y783A cells were serum starved for 72 h in F12 and plated on Fg (right) or Fn (left) in CCM1. Samples were assayed by crystal violet staining at the indicated times. Proliferation is plotted as the mean absorbance at 595 nm (A_{595}) ± SD from four independent experiments performed in triplicate. (C and D) CCM1 similarly promotes the G1–S transition in WT and Y783A cells on Fg. Serum-starved cells (time 0) were replated onto Fg in CCM1 as indicated and analyzed for cyclin D1 protein expression (C) and BrdU incorporation (D). (E and F) Growth of Y783A cells on Fg results in binucleation. Serum-starved cells were replated in wells coated with Fg, fixed at the indicated times, DAPI stained, and photographed. (E) Overlaid phase contrast and DAPI images of representative cells at growth day 4. Selected binucleated (red open arrowheads) and multinucleated (black open arrowhead) Y783A cells are indicated. Bar, 20 μm. (F) Plotted is the mean nuclear index calculated as the ratio of the total number of nuclei to the total number of cells (~100 cells/well) ± SD from three independent experiments. (G) Time-lapse analysis of cytokinesis of representative Y783A cells on Fg or Fn in CCM1. The rounding of cells that occurs early during mitosis was considered time 0. Bar, 25 μm. (H) Y783A cells attempt cytokinesis (scored as the appearance of the cleavage furrow) with similar kinetics as WT cells. Plotted is the mean percentage of attempts at 90-min intervals ± SD from three different fields (~100 cells/field) in a representative of three independent experiments. (I) Adenovirus-driven expression of the WT β3-1 chimera (Adβ3-1_{WT}) or plating cells on Fn restores cytokinesis. A cytokinesis success was scored as the separation and respreading of daughter cells within 1 h after mitotic rounding. At least 100 cells were analyzed per treatment. Results represent the mean ± SD of three independent experiments.

(Y783A cells) in the context of the αIIb-5β3-1 heterodimeric chimeric integrin. These chimeras contain the extracellular and transmembrane domain of the αIIbβ3 fibrinogen (Fg) receptor connected to the tails of the α5β1 fibronectin (Fn) receptor (Fig. 1 A), allowing CHO cell adhesion to Fg (Ylanne et al., 1993). We isolated the function of the recombinant chimeras by adhering cells to Fg in the serum-free growth medium CCM1 that does not support CHO cell proliferation in the absence of a preexisting matrix (unpublished data). WT cells showed robust proliferation on Fg in CCM1, whereas CHO K1 and Y783A cells proliferated poorly (Fig. 1 B). CCM1 similarly promoted proliferation of Y783A and CHO K1 cells on Fn (Fig. 1 B). Furthermore, infection of Y783A cells with an adenovirus that directed the expression of the β3-1 chimeric subunit containing the WT β1 tail restored cell proliferation of Y783A cells (unpublished data). Although Y783A cells show slow adhesion kinetics on Fg (Fig. S1 A, available at http://www.jcb.org/cgi/content/full/jcb.200603069/DC1), most cells adhere and spread

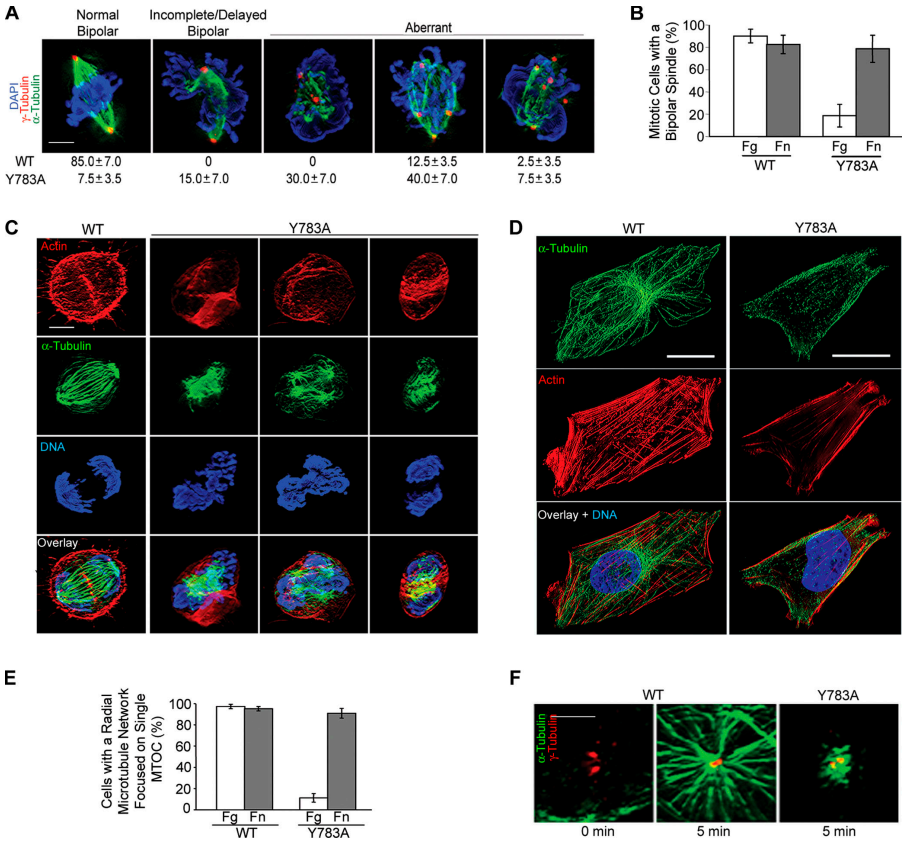

Figure 2. **Y783A cells adhered to Fg do not form a normal bipolar spindle at mitosis or a radial MT array focused at the centrosome during interphase.** (A) Serum-starved cells were replated on Fg-coated coverslips in CCM1. After 15–18 h, cells were immunostained as indicated. The percentage of WT and Y783A cells with each major phenotype is indicated below a representative image. Images were collected as z series for all three channels, similarly processed and deconvolved to generate 3D images. Results are the mean of three independent experiments (20 cells each) ± SD. Bar, 5 μm. (B) Quantification of bipolar spindles on Fg and Fn at metaphase and anaphase. A z series analysis was performed for each cell to confirm the number of spindle poles. Results are the mean of three independent experiments (25–50 cells each) ± SD. (C) Y783A cells show aberrant contractile rings at anaphase. Cells were also assayed at 18 h for the distribution of α-tubulin, actin, and DNA. Typical WT and Y783A cells at anaphase are shown. Bar, 10 μm. (D) The Y783A mutation inhibits formation of a radial MT network in interphase. Serum-starved cells were replated on Fg in CCM1 for 7 h, fixed, and stained as in C. Bars, 20 μm. (E) Quantification of the presence of a normal MT network at interphase in cells on Fg or Fn. Plotted is the mean ± SD from three independent experiments (100 cells each). (F) The Y783A mutation inhibits MT regrowth. Serum-starved cells were replated on Fg in CCM1, and MT regrowth was assayed at 14 h. At time 0, no MTs were focused on centrosomes (left). At 5 min, >95% of WT cells and <5% of Y783A cells showed MT regrowth (≥400 cells were analyzed). Similar results were obtained in three independent experiments. Images represent the best centrosome-containing plane from deconvolved z series that were similarly processed. Bar, 5 μm.

by 3 h (Fig. S1 B). Thus, the defect in proliferation is not simply due to a lack of adhesion.

Because anchorage-dependent cells require integrin signaling for entry into S phase (Assoian and Schwartz, 2001), we compared cyclin D1 induction and DNA synthesis in WT and Y783A cells. As expected, both were low in serum-starved cells. Surprisingly, cyclin D1 accumulation in Y783A cells at 7 h was equivalent to that in WT cells (Fig. 1 C). Furthermore, WT and Y783A cells incorporated similar levels of BrdU (Fig. 1 D). Thus, the proliferation defect is unlikely to be at the G1–S transition.

The poor proliferation of the Y783A cells was accompanied by accumulation of bi- and multinucleated cells (Fig. 1 E). Analysis of the binucleation kinetics revealed a uniform increase in the nuclei per cell in Y783A cells with no significant change in WT cells (Fig. 1 F). Because the most likely explanation was a defect in cytokinesis, we examined this process by time-lapse microscopy. After rounding at mitosis, WT cells completed cleavage furrow ingression within 5–10 min and cytokinesis within 20–30 min (unpublished data). In contrast, most Y783A cells attempting cytokinesis showed cleavage furrow regression and cytokinesis failure. This phenotype was suppressed when Y783A cells were adhered to Fn (Fig. 1, G and I). Quantification of cytokinesis attempts and successes during the first cell cycle on Fg in CCM1 indicated that ~90% of the WT cells attempted and successfully completed cytokinesis within 16–20 h (Fig. 1, H and I). A significant percentage of Y783A cells attempted cytokinesis, but most failed to divide (Fig. 1, H and I). Many Y783A cells showed a partially constricted cleavage furrow changing in diameter through an extended period of time and finally regressing to produce binucleated cells. In those few cases where cleavage furrow ingression was completed, midbody formation and/or daughter separation was significantly delayed or inhibited (unpublished data). As expected, Y783A cells successfully completed cytokinesis under the same conditions that promoted their proliferation (Fig. 1 H). Together, our data indicate that the Y783A mutation inhibits the successful completion of cytokinesis.

To gain mechanistic insight, we compared the actin and MT cytoskeletons in mitotic WT and Y783A cells that had proliferated on Fg in CCM1 for 15–18 h (a time of peak in cytokinesis attempts; Fig. 1 H). Cells at prometaphase/metaphase were identified by their round morphology and the presence of condensed chromosomes. At this stage, the majority of WT cells (85%) formed functional bipolar spindles, as judged by α- and γ-tubulin distribution and chromosome congression at the equatorial plane (Fig. 2 A). In contrast, most Y783A cells showed random distributions of chromosomes and multipolar spindles or no evidence of spindle assembly (Fig. 2 A). As expected, Y783A cells formed functional bipolar spindles on Fn (Fig. 2 B). At anaphase, WT cells showed normal contractile rings and chromosome segregation (Fig. 2 C); in contrast, most

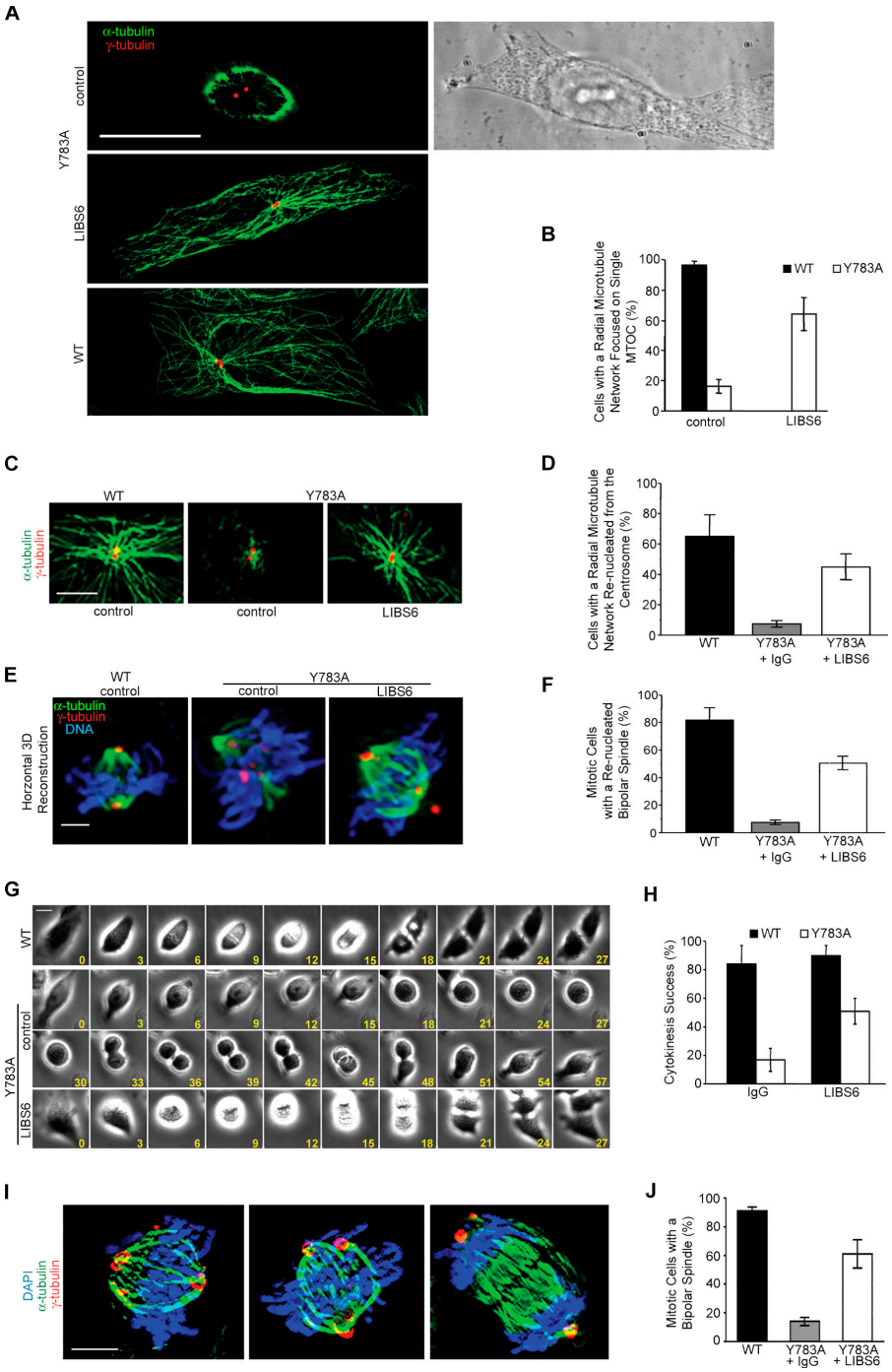

Figure 3. **LIBS6 restores the WT phenotype in Y783A cells adhered to Fg in CCM1.** (A and B) LIBS6 rescues a normal MT network at interphase. Serum-starved cells were replated on Fg in CCM1 in the presence of 150 ng/ml of either control IgG or LIBS6 for 4 h and then fixed and stained for α- and γ-tubulin. (A) Shown are images of representative cells. Bar, 20 μm. (B) Results are the mean percentage ± SD from three independent experiments (≥100 cells/treatment). (C and E) LIBS6 rescues MT regrowth at interphase and mitosis. Representative cells were imaged as described in Materials and methods. Bar, 5 μm. (D and F) Quantification of the rescue of MT regrowth from interphasic centrosomes and spindle poles. Results represent the mean ± SD from three independent experiments, each including 200 cells at interphase (D) and 25–50 mitotic cells (F). (G) Time-lapse comparison of cytokinesis in a representative WT (top), one of the common Y783A phenotypes in control IgG-treated cells (middle), and a typical rescue in LIBS6-treated Y783A cells (bottom). Cells were serum starved and harvested, and antibodies were added before the cells were replated on Fg. Time-lapse images were collected in 3-min intervals (bottom right on each image). The first image was considered time 0. Bar, 20 μm. (H) Quantification of the rescue of cytokinesis by LIBS6. A successful event was scored as described in Fig. 1 H. Results represent the mean ± SD from three independent experiments (≥50 cells/treatment were analyzed). (I) Rescue of bipolar spindles by LIBS6. Cells were processed as above. At 15–18 h, cells were fixed, stained, and analyzed as described in Fig. 2. Images correspond to representative prometaphase/metaphase and anaphase LIBS6-treated Y783A cells. Bar, 20 μm. (J) Quantification of the rescue of bipolar spindle by LIBS6. Presence of a bipolar spindle was determined as described in Fig. 2 A. Results represent mean ± SD from three independent experiments, each including 25–50 mitotic cells.

Y783A cells showed evidence of multiple contractile rings and a lack of chromosome segregation consistent with the presence of aberrant spindles (Fig. 2 C, middle). The few Y783A cells that were able to segregate chromosomes (Fig. 2 C, right) exhibited abnormalities at telophase (Fig. S2, available at http://www.jcb.org/cgi/content/full/jcb.200603069/DC1). Collectively, our data strongly suggest that the Y783A mutation inhibits cytokinesis by preventing the formation of a normal bipolar spindle.

To determine whether the defects were restricted to mitosis, we compared the MT cytoskeletons of Y783A and WT cells at interphase. WT cells had a complex array of numerous, long, distinct polymers originating from the centrosome and radiating to the cell cortex as expected (Fig. 2 D). In contrast, Y783A cells had fewer and more randomly organized MTs, which did not appear to emanate from the centrosome (Fig. 2 D). The Y783A phenotype was not due to decreases in expression of tubulin or surface chimeric integrins (Fig. S1, B and C). However, when we compared MT regrowth after nocodazole washout (Fry et al., 1998), we found that the regrowth of a radial MT array from the centrosome was clearly inhibited in Y783A cells (Fig. 2 F). These phenotypes were rescued when Y783A cells were adhered to Fn (Fig. 2 E and not depicted).

The Y783A mutation in the β1 tail is known to inhibit the expression of the high-affinity conformation of αIIb-5β3-1 in

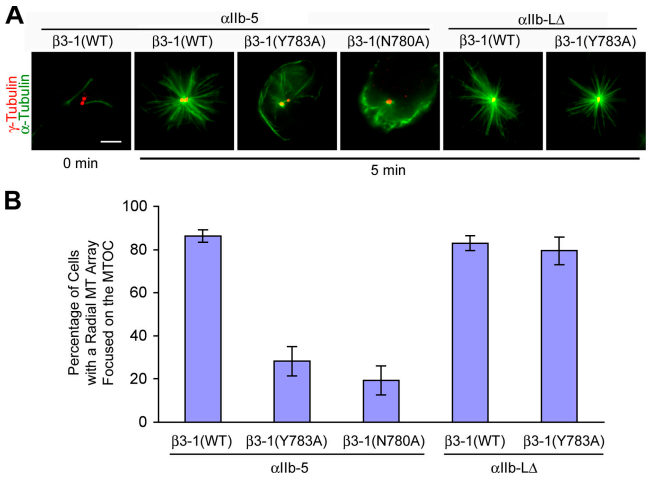

Figure 4. **Effect of activating and inactivating mutations on MT regrowth.** CHO K1 cells transiently expressing WT, Y783A, or N780A β1 tails in the context of either αIIb-5β3-1 or αIIb-LΔβ3-1 chimeric integrins were assayed for MT regrowth as described in Materials and methods. (A) Representative images are shown. Bar, 5 μm. (B) Quantification of MT regrowth. Results represent the mean ± SD from three independent experiments (≥300 cells/treatment).

CHO cells (O'Toole et al., 1995). Therefore, we tested whether LIBS6, a specific activating antibody for αIIbβ3 (Frelinger et al., 1991), could prevent the mutant phenotypes in Y783A cells. In control experiments, LIBS6 activated the Y783A chimeric integrin (unpublished data) and promoted rapid adhesion and spreading of Y783A cells on Fg (Fig. S1 D). Importantly, LIBS6 rescued the assembly of a radial MT network (Fig. 3, A and B), MT regrowth from centrosomes at interphase (Fig. 3, C and D) and spindle poles at mitosis (Fig. 3, E and F), the assembly of a bipolar spindle (Fig. 3, I and J), and cytokinesis (Fig. 3, G and H; and Videos 1–3, available at http://www.jcb.org/cgi/content/full/jcb.200603069/DC1). In agreement with these results, LIBS6 also prevented binucleation (unpublished data).

To determine whether the effects are specific for the Y783A mutation and the LIBS6 antibody, we tested additional mutations known to regulate integrin conformation (O'Toole et al., 1994, 1995). Coexpression of the αIIb-L deletion (αIIb-LΔ) with the β3-1(Y783A) chimeric subunit resulted in a constitutively active integrin (Fig. S2, D–F) and rescued MT regrowth (Fig. 4), as observed with LIBS6. In addition, coexpression of a β3-1 subunit containing an N780A mutation in the NPIY motif (β3-1[N780A]) with the αIIb-5 subunit prevented soluble Fg binding (Fig. S2, D–F) and inhibited MT regrowth (Fig. 4), mimicking the effects of the Y783A mutation. Thus, the inhibition and rescue of MT regrowth are not specific to the Y783A mutation and the LIBS6 activating antibody.

To demonstrate that the effects of the Y783A mutation were not specific to CHO cells or due to its expression in the context of the αIIb-5β3-1, we generated GD25 cell lines (β1-null; Fässler et al., 1995) expressing full-length human β1 containing either the WT (GD25 h-β1WT) or the Y783A mutant tail (GD25 h-β1Y783A; Fig. 5 A). In contrast, to the GD25 h-β1WT cells, MT regrowth from interphase centrosomes was inhibited in GD25 h-β1Y783A cells adhered to laminin-1 (Lm). Moreover, this phenotype was suppressed by TS2/16 (Masumoto and Hemler, 1993), a specific β1-activating antibody (Fig. 5, B and C). In addition, when these cells were mitotically arrested and replated on Lm, WT but not Y783A cells formed a normal bipolar spindle (Fig. 5, D and E). Thus, the effects of the Y783A mutation are not cell-type or integrin specific.

Our results provide the first evidence that integrins can regulate the assembly of the MT cytoskeleton during interphase and the bipolar spindle during mitosis and indicate that integrin activation is important for both. Previous studies demonstrated that the NPXY motif in β tails regulates activation by binding to talin (Tadokoro et al., 2003). Activating integrin antibodies circumvent the requirement for talin–β tail interactions in integrin activation (O'Toole et al., 1995). The ability of LIBS6 and TS2/16 to rescue the MT regrowth, bipolar spindle formation, and cytokinesis suggests that protein interactions with the NPIY motif, including talin binding, are not required downstream of integrin activation to regulate these processes. These antibodies may promote the association of integrins with other receptors and/or the interaction of the tail with cytoskeletal or signaling proteins to regulate the MT cytoskeleton.

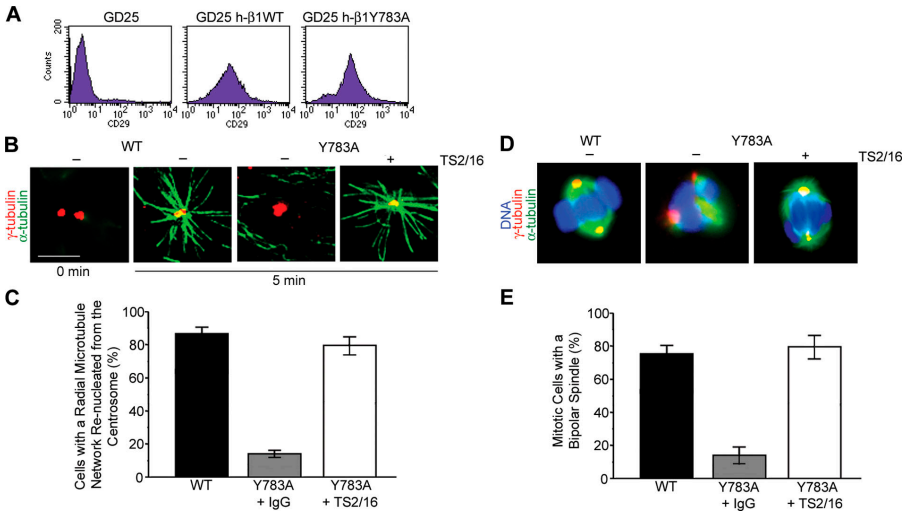

Figure 5. **Expression of the Y783A mutation in the context of the full-length human β1 subunit in β1-null GD25 cells.** (A) WT and Y783A β1 are expressed at similar levels in stable transfectants as assayed by flow cytometry using mAb K20. (B and C) Inhibition and rescue of MT assembly in GD25 h-β1Y783A cells. MT regrowth was assayed in CCM1 ± TS2/16 (10 μg/ml). (B) Representative images are shown. (C) Plotted is mean ± range from two independent experiments (≥200 cells/treatment). (D and E) Inhibition and rescue of bipolar spindle formation. GD25 h-β1Y783A cells proliferating in serum-containing medium were arrested in mitosis with nocodazole and replated on Lm-coated coverslips in CCM1. At 30–45 min, cells were fixed and processed for spindle analysis. (D) Shown are representative images of WT and Y783A ± TS2/16. (E) Results represent the mean ± range from two independent experiments (≥25 cells/treatment). Bar, 5 μm.

MT dynamics are under tight and complex control throughout the cell cycle. At interphase, the organization of the MT network requires the regulation of MT nucleation, growth, and anchorage at the centrosome and the association of MTs with the cell cortex. The assembly of the bipolar spindle at mitosis also requires the regulation of kinetochore-associated MTs, as well as centrosome duplication and cohesion (Doxsey, 2001; Gadde and Heald, 2004; Kline-Smith and Walczak, 2004; Maiato et al., 2004). The Y783A mutation may inhibit the activity of one or more of the proteins that regulate these events. The goal of future studies will be to identify the aspects and targets of integrin function required for spindle assembly and cytokinesis.

Materials and methods

Cell culture

CHO K1, WT, and Y783A CHO cell lines were cultured in F12 medium ± 10% FBS or CCM1 (Hyclone). WT and Y783A-GD25 cells were cultured in DME + 10% FBS or CCM1 as indicated. The generation of stable CHO and GD25 cell lines is described in the supplemental text (available at http://www.jcb.org/cgi/content/full/jcb.200603069/DC1). Transient transfection of CHO K1 cells was performed using the Mojo transfection reagent (Mirus). Where indicated, cells were serum starved in F12 or DME and replated on the indicated matrices. For binucleation and cytoskeletal analysis, $\sim 5 \times 10^4$ cells were replated in CCM1 in 24-well dishes on 15 μg/ml Fg/Fn (CHO cells) or 30 μg/ml Lm (GD25 cells) and processed as described in the figure legends.

Cell proliferation assays

Serum-starved cells were replated onto either Fg- or Fn-coated (15 μg/ml) 12-well dishes (3×10^3 cells/well, in triplicate), fixed at the indicated times in 3.7% paraformaldehyde, and stained with crystal violet (0.5% in 20% methanol) for 1 h at room temperature. Incorporated dye was extracted with 1% SDS and quantified by measuring A_{598} in a spectrophotometer. To assay DNA synthesis, serum-starved cells and serum-starved cells replated on Fg in CCM1 for 5 h were supplemented with BrdU for 18 h. Cells positive for BrdU incorporation were quantified by microscopy.

MT regrowth

Serum-starved cells ($\sim 5 \times 10^4$) were replated on 15 μg/ml of either Fg or Fn (CHO cells) or on 30 μg/ml Lm (GD25 cells) in CCM1. 3–14 h after plating, cells were treated with 10 μg/ml nocodazole (Calbiochem) for 2 h at 4°C, washed with cold PBS to remove the drug, allowed to nucleate MTs for 5–15 min in warmed CCM1 ± LIBS6 (CHO cells) or TS2/16 (GD25 cells), and processed for immunofluorescence microscopy.

Time-lapse microscopy

Serum-starved cells were replated (24-well dishes) on Fg or Fn in CCM1 supplemented with 10 mM Hepes, pH 7.4. 3 h after seeding, when most cells were fully spread, dishes were transferred to a microscope equipped with a heated (37°C) chamber, and phase-contrast images were recorded (12 frames/h) during the first cell cycle (16–20 h). Multiple fields (three per sample) were analyzed using a rotary stage and 20× objective. Where indicated, cells were arrested at metaphase by nocodazole treatment, isolated, replated on Fn or Fg in CCM1 ± LIBS6, and imaged as before but at 2 frames/min to analyze cytokinesis in greater detail.

Immunofluorescence microscopy

Cells were permeabilized for 30 s in 80 mM Pipes, pH 6.8, 5 mM EGTA, 1 mM $MgCl_2$, and 0.5% Triton X-100; fixed for 10 min in the same buffer containing 5% glutaraldehyde; and incubated for 7 min in 1% sodium borohydrate in PBS. To coanalyze MTs and F-actin, cells were fixed in 3.7% paraformaldehyde and 1% sucrose in PBS for 5 min, permeabilized in PBS and 0.5% Triton X-100 for 10 min, and processed for immunostaining as glutaraldehyde-fixed cells (excluding the glutaraldehyde-quenching step). The following antibodies were used: α-tubulin (mouse mAb DM1A; Sigma-Aldrich), γ-tubulin (rabbit AK-15; Sigma-Aldrich), Alexa Fluor 488–conjugated goat anti-mouse (Invitrogen), and Alexa Fluor 594–conjugated goat anti-rabbit (Invitrogen). F-actin was analyzed with Alexa Fluor 594–conjugated Phalloidin (1:300 dilution), and DNA was stained with 1 μM of either Hoechst 33342 or DAPI (Invitrogen). Samples were analyzed using an inverted microscope (TE2000-E; Nikon) equipped with phase contrast and epifluorescence, a digital camera (CoolSNAP HQ; Roper Scientific), a Ludl rotary encoded stage, 37°C incubator, and MetaVue (Molecular Devices) and AutoQuant deconvolution software (AutoQuant Imaging, Inc.).

Western blotting

Protein expression was analyzed by Western blotting using the following commercially available antibodies: α-tubulin (mouse mAb DM1A), cyclin D1 (mouse mAb DCS-6; BD Biosciences), Pan ERK (mouse mAb 16; BD Biosciences), and cyclin B1 (mouse mAb GNS1; Santa Cruz Biotechnology, Inc.). Blots were stripped and reprobed with the indicated antibodies for loading controls.

Online supplemental material

The supplemental text provides information relating to the generation of chimeric integrins and stable cell lines. Fig. S1 shows the adhesion and spreading of WT and Y783A cells on Fg in CCM1, expression levels of α-tubulin and chimeric integrins under these conditions, and the promotion of rapid adhesion and spreading of Y783A cells on Fg by LIBS6. Fig. S2 shows the characteristic telophase phenotypes in these cells under similar conditions (S2A-C), as well as the characterization of the ability of CHO cells transiently expressing WT and mutant chimeric integrins to bind soluble and immobilized Fg (S2D-G). Videos 1 and 2 show the completion and failure of the cytokinesis in WT and Y783A cells, respectively, on Fg in CCM1. Videos 3 and 4 show the rescue of cytokinesis in Y783A cells on Fn or on Fg when treated with LIBS6, respectively. Online supplemental material is available at http://www.jcb.org/cgi/content/full/jcb.200603069/DC1.

We thank Dr. M.H. Ginsberg for the αIIb, β3, and αIIb-LΔ expression vectors and the LIBS6 antibody; Dr. S. Blystone for the 7G2 antibody; Dr. R. Fässler for the GD25 cells; Dr. Y. Takada for human β1 cDNA; Drs. J. Sottile, A. Khodjakov, and Dr. K.M. Yamada for critically reading this manuscript; and Dr. A. Khodjakov for advise in imaging MTs.

This work was supported by National Institutes of Health grants GM51540 (to S.E. LaFlamme) and T32-HL07194 (to C.G. Reverte) and by the American Heart Association postdoctoral fellowship 0525875T (to C.G. Reverte).

Submitted: 14 March 2006
Accepted: 10 July 2006

References

Assoian, R.K., and M.A. Schwartz. 2001. Coordinate signaling by integrins and receptor tyrosine kinases in the regulation of G1 phase cell-cycle progression. *Curr. Opin. Genet. Dev.* 11:48–53.

Aszodi, A., E.B. Hunziker, C. Brakebusch, and R. Fässler. 2003. Beta1 integrins regulate chondrocyte rotation, G1 progression, and cytokinesis. *Genes Dev.* 17:2465–2479.

Ben-Ze'ev, A., and A. Raz. 1981. Multinucleation and inhibition of cytokinesis in suspended cells: reversal upon reattachment to a substrate. *Cell.* 26:107–115.

Bodeau, A.L., A.L. Berrier, A.M. Mastrangelo, R. Martinez, and S.E. LaFlamme. 2001. A functional comparison of mutations in integrin beta cytoplasmic domains: effects on the regulation of tryosine phosphorylation, cell spreading, cell attachment and beta1 integrin conformation. *J. Cell Sci.* 114:2795–2807.

Doxsey, S. 2001. Re-evaluating centrosome function. *Nat. Rev. Mol. Cell Biol.* 2:688–698.

Fässler, R., M. Pfaff, J. Murphy, A.A. Noegel, S. Johansson, R. Timpl, and R. Albrecht. 1995. Lack of β1 integrin gene in embryonic stem cells affects morphology, adhesion, and migration but not integration into the inner cell mass of blastocysts. *J. Cell Biol.* 128:979–988.

Frelinger, A.L., III, X.P. Du, E.F. Plow, and M.H. Ginsberg. 1991. Monoclonal antibodies to ligand-occupied conformers of integrin alpha IIb beta 3 (glycoprotein IIb-IIIa) alter receptor affinity, specificity, and function. *J. Biol. Chem.* 266:17106–17111.

Fry, A.M., P. Meraldi, and E.A. Nigg. 1998. A centrosomal function for the human Nek2 protein kinase, a member of the NIMA family of cell cycle regulators. *EMBO J.* 17:470–481.

Gadde, S., and R. Heald. 2004. Mechanisms and molecules of the mitotic spindle. *Curr. Biol.* 14:R797–R805.

Geiger, B., A. Bershadsky, R. Pankov, and K.M. Yamada. 2001. Transmembrane crosstalk between the extracellular matrix–cytoskeleton crosstalk. *Nat. Rev. Mol. Cell Biol.* 2:793–805.

Glotzer, M. 2001. Animal cell cytokinesis. *Annu. Rev. Cell Dev. Biol.* 17:351–386.

Hynes, R.O. 2002. Integrins: bidirectional, allosteric signaling machines. *Cell.* 110:673–687.

Kline-Smith, S.L., and C.E. Walczak. 2004. Mitotic spindle assembly and chromosome segregation: refocusing on microtubule dynamics. *Mol. Cell.* 15:317–327.

Maddox, A.S., and K. Burridge. 2003. RhoA is required for cortical retraction and rigidity during mitotic cell rounding. *J. Cell Biol.* 160:255–265.

Maiato, H., C.L. Rieder, and A. Khodjakov. 2004. Kinetochore-driven formation of kinetochore fibers contributes to spindle assembly during animal mitosis. *J. Cell Biol.* 167:831–840.

Masumoto, A., and M.E. Hemler. 1993. Multiple activation states of VLA-4. Mechanistic differences between adhesion to CS1/fibronectin and to vascular cell adhesion molecule-1. *J. Biol. Chem.* 268:228–234.

Orly, J., and G. Sato. 1979. Fibronectin mediates cytokinesis and growth of rat follicular cells in serum-free medium. *Cell.* 17:295–305.

O'Toole, T.E., Y. Katagiri, R.J. Faull, K. Peter, R. Tamura, V. Quaranta, J.C. Loftus, S.J. Shattil, and M.H. Ginsberg. 1994. Integrin cytoplasmic domains mediate inside-out signal transduction. *J. Cell Biol.* 124:1047–1059.

O'Toole, T.E., J. Ylanne, and B.M. Culley. 1995. Regulation of integrin affinity states through an NPXY motif in the beta subunit cytoplasmic domain. *J. Biol. Chem.* 270:8553–8558.

Tadokoro, S., S.J. Shattil, K. Eto, V. Tai, R.C. Liddington, J.M. de Pereda, M.H. Ginsberg, and D.A. Calderwood. 2003. Talin binding to integrin beta tails: a final common step in integrin activation. *Science.* 302:103–106.

Vandre, D.D., P. Kronebusch, and G.G. Borisy. 1984. The interphase-motisis transition: microtubule rearrangements in cultured cells and sea urchin eggs. *In* Molecular Biology of the Cytoskeleton. G.G. Borisy, D.W. Cleveland, and D.B. Murphy, editors. Cold Spring Harbor Laboratory Press, Cold Spring Harbor, NY. 3–16.

Winklbauer, R. 1986. Cell proliferation in the ectoderm of the *Xenopus* embryo: development of substratum requirements for cytokinesis. *Dev. Biol.* 118:70–81.

Ylanne, J., Y. Chen, T.E. O'Toole, J.C. Loftus, Y. Takada, and M.H. Ginsberg. 1993. Distinct functions of integrin α and β subunit cytoplasmic domains in cell spreading and formation of focal adhesions. *J. Cell Biol.* 122:223–233.